Lie Group Approach to Dynamic-Model-Aided Navigation of Multirotor Unmanned Aerial Vehicles

NAK YONG KO [1], (Member, IEEE), **GYEONGSUB SONG** [2],
WONKEUN YOUN [3], (Member, IEEE), AND **SUNG HYUN YOU** [4]

[1]Department of Electronic Engineering, Interdisciplinary Program in IT-Bio Convergence Systems, Chosun University, Gwangju 61452, South Korea
[2]Department of Control and Instrumentation Engineering, Interdisciplinary Program in IT-Bio Convergence Systems, Chosun University, Gwangju 61452, South Korea
[3]Department of Autonomous Vehicle System Engineering, Chungnam National University, Daejeon 34134, South Korea
[4]Department of Electronic Engineering, Chosun University, Gwangju 61452, South Korea

Corresponding author: Sung Hyun You (you@chosun.ac.kr)

ABSTRACT In this study, the Lie group approach was used for state estimation of the dynamic-model-aided navigation (DMAN) of a small multirotor unmanned aerial vehicle. The unit quaternions constituting a Lie group called the three-sphere space (S^3) were used to represent the attitude in the dynamic equations for the process and measurement models. The linearization of these models is presented in terms of Lie algebra corresponding to S^3. The use of Lie algebra to describe the attitude increment conforms to the linearity assumption, on which the measurement update of the extended Kalman filter (EKF) is based. In this study, it was experimentally validated that the Lie group approach combined with DMAN performs better than the EKF that uses the conventional linearization of the process and measurement models under the assumption that the nonlinearity effect is negligible for a small attitude increment. It was demonstrated that the navigation states estimated using the proposed model are better than or comparable to those obtained using the current methods, and the proposed method significantly improves the internal properties.

INDEX TERMS Three-sphere space, Lie group, Lie algebra, unit quaternion, multirotor, navigation, dynamic model, Kalman filter.

I. INTRODUCTION

Many vehicle attitude representations are difficult to use because they do not constitute a linear space. This is the case with operations on attitude such as differentiation, integration, and calculation of covariance that are involved in Kalman filtering [1], [2]. The attitude forms a three-dimensional special orthogonal group (SO(3)), three-sphere space (S^3), and two-dimensional special unitary group (SU(2)), rather than a linear space [3], [4]. This non-linearity complicates attitude estimation using an approach based on the assumption that the variables and operations are in a linear space, or that linearization does not cause any significant problems. Kalman filter (KF) approaches to attitude estimation also suffer from this non-linearity. Therefore, this

The associate editor coordinating the review of this manuscript and approving it for publication was Cong Pu [ID].

study proposed utilizing Lie group theory, whereby a KF is used for attitude estimation in terms of unit quaternions. Specifically, an extended KF (EKF) was used in S^3 for the dynamic-model-aided navigation (DMAN) of a small quadrotor.

Lie theory has been used in the application of KFs, either explicitly or implicitly. Multiplicative EKFs (MEKFs) implicitly employ Lie theory, where the attitude error is represented by a three-component error vector [5]–[7]. The three-component error vectors constitute Lie algebra corresponding to a Lie group composed of unit quaternions. Although not explicitly expressed, the multiplicative term in an MEKF corresponds to the exponential of the Lie algebra element, called the three-component error vector [5]. In contrast, invariant EKFs (IEKFs) explicitly use Lie theory to handle nonlinear and norm-preserving quaternion attitude representations [8]–[10], which ensures robust performance

and improved convergence [11]. The performance improvement brought about by matrix Lie group formulation in solving an attitude control problem [9] has been demonstrated by numerical analysis. However, neither MEKFs nor IEKFs have previously been used for DMAN.

The matrix Lie group of double direct isometries, $SE_2(3)$, in which the attitude, position, and velocity are described by a 5×5 matrix, was explored for estimation and control. In [12], it was verified that the use of matrix Lie group $SE_2(3)$ theory facilitates accurate propagation of uncertainty and exact pre-integration of the inertial measurement unit (IMU). This provides the background theory and tools of $SE_2(3)$ for estimation and control applications. Cohen *et al.* defined a matrix Lie group to represent a set of state variables that included sensor biases and wind velocity, as well as attitude, velocity, and position [13]. The defined matrix Lie group contained $SE_2(3)$, in which the navigation state variables of attitude, velocity, and position evolve. References [14] and [15] proposed nonlinear observers on matrix Lie group $SE_2(3)$ that estimated the attitude, position, and velocity using landmark measurements in addition to inertial measurements. The use of Lie group theory efficiently handled measurement noise and improved stability.

Many KF applications that have utilized Lie group theory used matrix Lie groups [16]–[18]. Reference [19] implemented an EKF on the Lie group of the special orthogonal group SO(3) to estimate the initial attitude of the IMU relative to a navigation coordinate system. In [17], a general framework for the application of KFs in matrix Lie groups was presented, and in [18], KFs were applied to matrix Lie groups for simultaneous localization and mapping with simulation results. In contrast to the aforementioned studies, the Lie group approach is used in the S^3 space in this study. Moreover, this study focused on a practical application: DMAN of a multirotor unmanned aerial vehicle (UAV).

The unit quaternions representing the vehicle attitude or rotation constitute a Lie group called the three-sphere space [20]. Increments are evaluated in the tangent space, which is called Lie algebra $\mathfrak{s}^3$, for prediction and measurement updates. The adjustment for the measurement update, which is the product of the Kalman gain and measurement innovation, is derived in Lie algebra. This correction restores the Lie group quantity from the adjustment represented in terms of Lie algebra. Covariance is calculated using Lie algebra. The states are in the Lie group, and the difference between the states and covariance is evaluated using Lie algebra. Lie group theory enables the evaluation of the state error, noise, and increment without a linear approximation. In [21], a nonlinear state error was defined in the Lie group for strapdown inertial navigation systems with a miniature IMU, global navigation satellite system (GNSS), and magnetometer.

This paper describes the use of Lie group theory for dynamic-model-aided navigation of multirotor unmanned aerial vehicles. To the best of the authors' knowledge, there has been no research on the use of the Lie group approach for dynamic-model-aided estimation of a multirotor navigation system. The proposed method employs EKF for the estimation. The Lie group approach is appropriate for use in EKF; it facilitates the differentiation of the process model and measurement model that is required to derive the Jacobian matrix for EKF implementation.

The Lie group approach is applicable to the unscented Kalman filter (UKF) [22]–[25] and cubature Kalman filter (CKF) [26]. However, the application of Lie group theory for the UKF or CKF requires additional computations to make the approach compatible with Lie group theory. Additions and subtractions of sigma points involve the computation of exponentials and logarithms [23]. The weighted mean calculated by the usual addition and subtraction method does not produce a proper Lie group element. Therefore, calculation of the weighted mean requires the repeated calculation of exponentials for the Lie algebra elements and logarithms for the Lie group elements. To reduce computational complexity, a method utilizing an optimum regression matrix has been proposed [22].

Dynamic-model-aided navigation is essential for UAVs when a global navigation satellite system (GNSS) is temporarily unavailable or unstable [27]–[29]. In [27], an EKF was used for the DMAN of a quadrotor; however, an approach involving S^3 was not adopted. In contrast to the model used in that study, the proposed measurement model includes the geomagnetic field as a measurement variable. Furthermore, the noise involved in attitude propagation is described in terms of Lie algebra.

The novelty and features of the proposed approach are as follows.

1) Lie group theory is used for dynamic-model-aided estimation of a multirotor UAV navigation system.
2) Using Lie group theory for dynamic-model-aided estimation improves the performance of the estimation, that is, improvement in the convergence of Kalman gain and measurement innovation and the estimation accuracy.
3) Lie group three-sphere space S^3 is used for estimation; however, many previous Lie group approaches adopted matrix Lie groups. S^3 consists of four components, whereas matrix Lie group SO(3) uses nine components.
4) Jacobians of the process model and measurement model are derived using Lie group theory.

Section II describes the process and measurement models, in which a dynamic model of the quadrotor is incorporated for the estimation. In Section III, the Lie group approach is presented, and Jacobians are derived for the implementation of the EKF in S^3 based on Lie theory. Section IV describes the experiments and results demonstrating the improvements owing to the proposed method compared with the previous applications of KFs in DMAN [27]. Section V concludes the paper.

II. PROCESS AND MEASUREMENT EQUATIONS INCORPORATING THE DYNAMIC MODEL

The process and measurement equations are established and extended based on [27]. This section summarizes the models used for the Lie-theory-based derivations in Section III.

A. NOMENCLATURE

Throughout this paper, the following notations are used:

$x(t)$ location at time t in the local north-east-down (NED) coordinate frame; $x(t) = \begin{bmatrix} x(t) & y(t) & z(t) \end{bmatrix}^T$

$\tilde{z}(t)$ altitude measured by a barometric altimeter at time t

$v(t)$ velocity at time t in the local NED coordinate frame; $v(t) = \begin{bmatrix} v_x(t) & v_y(t) & v_z(t) \end{bmatrix}^T$

${}^b v(t)$ velocity at time t in the vehicle coordinate frame; ${}^b v(t) = \begin{bmatrix} {}^b v_x(t) & {}^b v_y(t) & {}^b v_z(t) \end{bmatrix}^T$

$q(t)$ attitude at time t in the local NED coordinate frame represented by a unit quaternion; $q(t) = \begin{bmatrix} q_w(t) & q_x(t) & q_y(t) & q_z(t) \end{bmatrix}^T = \begin{bmatrix} q_w(t) & \vec{q}(t) \end{bmatrix}^T \in S^3$, where $\vec{q}(t) = \begin{bmatrix} q_x(t) & q_y(t) & q_z(t) \end{bmatrix}^T$

$q^*(t)$ conjugate of the quaternion $q(t)$; $q^*(t) = \begin{bmatrix} q_w(t) & -\vec{q}(t) \end{bmatrix}^T$

$\omega(t)$ angular rate at time t in the local sensor coordinate frame; $\omega(t) = \begin{bmatrix} \omega_x(t) & \omega_y(t) & \omega_z(t) \end{bmatrix}^T$

$\tilde{\omega}(t)$ measured angular rate at time t in the local sensor coordinate frame; $\tilde{\omega}(t) = \begin{bmatrix} \tilde{\omega}_x(t) & \tilde{\omega}_y(t) & \tilde{\omega}_z(t) \end{bmatrix}^T$

g gravitational acceleration (m/s²)

Δt_i time difference between the $(i-1)$-th and i-th time sequence; $\Delta t_i = t_i - t_{i-1}$

$r_k(t)$ rotation speed of the k-th propeller at time t in revolutions per minute (RPM)

$\mathfrak{f}_k(t)$ thrust force generated by the k-th propeller with rotation speed $r_k(t)$

$\mathfrak{t}_k(t)$ torque generated by the k-th propeller with rotation speed $r_k(t)$

m mass of the quadrotor

$a_r(t)$ acceleration generated by the four propellers at time t in the z-direction of the vehicle; $a_r(t) = \begin{bmatrix} 0 & 0 & \frac{1}{m} \sum_{k=1}^{4} \mathfrak{f}_k(t) \end{bmatrix}^T$

$a(t)$ acceleration of the vehicle at time t in the local NED coordinate frame; $a(t) = \begin{bmatrix} a_x(t) & a_y(t) & a_z(t) \end{bmatrix}^T$

$\tilde{a}(t)$ acceleration measured by using the accelerometer of an IMU or attitude and heading reference system (AHRS); $\tilde{a}(t) = \begin{bmatrix} \tilde{a}_x(t) & \tilde{a}_y(t) & \tilde{a}_z(t) \end{bmatrix}^T$

$\tilde{m}(t)$ geomagnetic field measured by using a magnetometer; $\tilde{m}(t) = \begin{bmatrix} \tilde{m}_x(t) & \tilde{m}_y(t) & \tilde{m}_z(t) \end{bmatrix}^T$

$\hat{\mathbf{x}}(t_i|t_{i-1})$ *a priori* estimation of the variable $\mathbf{x}(t)$ at time $t = t_i$

$\hat{\mathbf{x}}(t_i)$ *a posteriori* estimation of the variable $\mathbf{x}(t)$ at time $t = t_i$

$P(t_i)$ error covariance matrix of the estimate $\hat{\mathbf{x}}(t_i)$ at time $t = t_i$

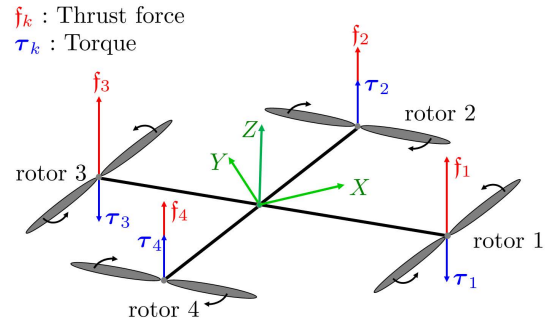$\mathfrak{f}_k$: Thrust force
τ_k : Torque

FIGURE 1. Coordinate system for quadrotor UAVs.

M^k the k-th column of the matrix M

$\otimes$ operator that multiplies two quaternions; to multiply a vector $\vec{n} \in R^3$ and a quaternion, the vector is augmented to the pure quaternion $\begin{bmatrix} 0 & \vec{n} \end{bmatrix}^T$

$[p]_\times$ cross product matrix of a vector p; $p \times r = [p]_\times r$ for two vectors $p \in R^3$ and $r \in R^3$

$R(q(t))$ rotation matrix corresponding to the rotation by a quaternion $q(t)$; $R(q(t))p = q(t) \otimes p \otimes q^*(t)$ for a vector $p \in R^3$

$R(r)$ rotation matrix representing the rotation by the rotation vector r; $r = \frac{r}{\|r\|} \|r\|$, where $\|r\|$ is the rotation angle, and $\frac{r}{\|r\|}$ is the axis of rotation

I_m identity matrix with dimension $m \times m$

0_m zero matrix with dimension $m \times m$

I_{xx} moment of inertia in the x direction. Similarly, I_{yy} and I_{zz} are the moments of inertia in the y and the z direction, respectively

In this study, the local NED coordinate frame was regarded as the reference coordinate frame. The dynamic model, process equation, and measurement equation were derived based on the vehicle coordinate system shown in Fig. 1. The sensor coordinate system was set such that it coincided with the vehicle coordinate system, and there was no need to convert the sensor measurements to values in the vehicle coordinate system.

For notational convenience, the time index t_i within parentheses is denoted by subscript i (e.g., P_i is used instead of $P(t_i)$, and $\hat{\mathbf{x}}_{i|i-1}$ is used instead of $\hat{\mathbf{x}}(t_i|t_{i-1})$).

B. PROCESS EQUATIONS

The position, velocity, and attitude of a UAV are to be estimated. The state $\mathbf{x}(t)$ at time t includes the angular rate of the vehicle motion as well as its position, velocity, and attitude to facilitate the estimation, as follows:

$$\mathbf{x}(t) = \begin{bmatrix} x(t) & v(t) & q(t) & \omega(t) \end{bmatrix}^T. \quad (1)$$

The process equation describes the time derivative of the state as a function $f(\cdot)$ of the state $\mathbf{x}(t)$ and input $u(t)$:

$$\dot{\mathbf{x}}(t) = f(\mathbf{x}(t), u(t)), \quad (2)$$

where $u(t) = \begin{bmatrix} r_1(t) & r_2(t) & r_3(t) & r_4(t) \end{bmatrix}^T$. The process equation $f(\mathbf{x}(t), u(t))$ is based on the dynamic model of

a quadrotor described in [30], and the details of the derivation are provided in [27].

The time derivatives of position and velocity are as follows:

$$\dot{\boldsymbol{x}}(t) = \boldsymbol{v}(t), \tag{3}$$

$$\dot{\boldsymbol{v}}(t) = \begin{bmatrix} 0 & 0 & g \end{bmatrix}^T + \boldsymbol{R}(q(t))\boldsymbol{a}_r(t)$$
$$+ \boldsymbol{R}(q(t))\left\{ \boldsymbol{V}(t)\,\boldsymbol{R}^T(q(t))\boldsymbol{v}(t) \right\}. \tag{4}$$

In (4), the drag force ratio matrix $\boldsymbol{V}(t)$ and drag force coefficient $k_l(t)$ of the quadrotor are expressed as follows:

$$\boldsymbol{V}(t) = \begin{bmatrix} -k_l(t) & 0 & 0 \\ 0 & -k_l(t) & 0 \\ 0 & 0 & 0 \end{bmatrix}, \tag{5}$$

$$k_l(t) = \frac{1}{m}\lambda_1 \sum_{k=1}^{4} r_k(t). \tag{6}$$

In (6), λ_1 denotes the drag coefficient of the propeller [28]. In (4), $\boldsymbol{R}(q(t))\boldsymbol{a}_r(t)$ and $\boldsymbol{R}(q(t))\left\{\boldsymbol{V}(t)\,\boldsymbol{R}^T(q(t))\,\boldsymbol{v}(t)\right\}$ describe the dynamics of the quadrotor.

The time derivative of the quaternion that represents the attitude of a vehicle is obtained using (7), and the derivative of the angular rate is obtained using (8).

$$\dot{q}(t) = \frac{1}{2}q(t) \otimes \boldsymbol{\omega}(t), \tag{7}$$

$$\dot{\boldsymbol{\omega}}(t) = \begin{bmatrix} \dfrac{I_{yy}-I_{zz}}{I_{xx}}\omega_y(t)\,\omega_z(t) \\[6pt] \dfrac{I_{zz}-I_{xx}}{I_{yy}}\omega_x(t)\,\omega_z(t) \\[6pt] \dfrac{I_{xx}-I_{yy}}{I_{zz}}\omega_x(t)\,\omega_y(t) \end{bmatrix} + \begin{bmatrix} \dot{\omega}_{x\mathfrak{f}}(t) \\[4pt] \dot{\omega}_{y\mathfrak{f}}(t) \\[4pt] \dot{\omega}_{z\mathfrak{t}}(t) \end{bmatrix}, \tag{8}$$

where

$$\dot{\omega}_{x\mathfrak{f}}(t) = \frac{1}{I_{xx}}\left\{ d_{23}(\mathfrak{f}_2(t)+\mathfrak{f}_3(t)) - d_{14}(\mathfrak{f}_1(t)+\mathfrak{f}_4(t)) \right\},$$

$$\dot{\omega}_{y\mathfrak{f}}(t) = \frac{1}{I_{yy}}\left\{ d_{34}(\mathfrak{f}_3(t)+\mathfrak{f}_4(t)) - d_{12}(\mathfrak{f}_1(t)+\mathfrak{f}_2(t)) \right\},$$

$$\dot{\omega}_{z\mathfrak{t}}(t) = \frac{1}{I_{zz}}\left\{ -\mathfrak{t}_1(t) + \mathfrak{t}_2(t) - \mathfrak{t}_3(t) + \mathfrak{t}_4(t) \right\}.$$

In (8), d_{ij} ($ij \in \{12, 23, 34, 14\}$) is the distance from the origin of the vehicle coordinate frame to the line connecting the centers of propellers i and j. The distance is projected onto the xy plane of the vehicle coordinate frame.

The process equation of quadrotor motion for the application of the EKF consists of (3), (4), (7), and (8). Equations (4) and (8) include a dynamic model that involves the thrust force and torque exerted by the propellers, which play a key role in aiding navigation.

C. MEASUREMENT MODEL

The measurement $z(t)$ consists of the acceleration $\tilde{\boldsymbol{a}}(t)$, acceleration direction $\boldsymbol{d}_a(t)$, geomagnetic field direction $\boldsymbol{d}_m(t)$, angular rate $\tilde{\boldsymbol{\omega}}(t)$, and altitude $\tilde{z}(t)$.

$$z(t) = \begin{bmatrix} \tilde{\boldsymbol{a}}(t) & \boldsymbol{d}_a(t) & \boldsymbol{d}_m(t) & \tilde{\boldsymbol{\omega}}(t) & \tilde{z}(t) \end{bmatrix}^T. \tag{9}$$

The acceleration and angular rate were measured using an IMU or AHRS, and the geomagnetic field was measured using the magnetometer in the AHRS. Altitude was measured using a barometric altimeter. The measurement $z(t)$ has 13 elements.

The measurement model describes $z(t)$ as a function of the state $\mathbf{x}(t)$, input $\boldsymbol{u}(t)$, and measurement noise $\boldsymbol{n}_m(t)$ as follows:

$$z(t) = \boldsymbol{h}(\mathbf{x}(t), \boldsymbol{u}(t)) + \boldsymbol{n}_m(t),$$
$$\boldsymbol{n}_m(t) \sim \mathcal{N}(0, \boldsymbol{Q}_m(t)). \tag{10}$$

The measurement equations $\boldsymbol{h}(\mathbf{x}(t), \boldsymbol{u}(t))$ are derived as described below. The measurement equations for the acceleration $\tilde{\boldsymbol{a}}(t)$, angular rate $\tilde{\boldsymbol{\omega}}(t)$, and altitude $\tilde{z}(t)$ are the same as those in [27].

The acceleration measurement is related to two state variables: velocity and attitude. It is also related to the thrust force exerted by the propellers. Thus, the measurement equation for acceleration $\tilde{\boldsymbol{a}}(t) = \begin{bmatrix} \tilde{a}_x(t) & \tilde{a}_y(t) & \tilde{a}_z(t) \end{bmatrix}^T$ is as follows:

$$\tilde{\boldsymbol{a}}(t) = \boldsymbol{\Lambda}(t)\left\{ q^*(t) \otimes \boldsymbol{v}(t) \otimes q(t) \right\} + \mathfrak{f}(t), \tag{11}$$

where

$$\boldsymbol{\Lambda}(t) = -k_l(t)\begin{bmatrix} 1 & 0 & 0 \\ 0 & 1 & 0 \\ 0 & 0 & 0 \end{bmatrix},$$

$$\mathfrak{f}(t) = \boldsymbol{a}_r(t).$$

In (11), $\boldsymbol{\Lambda}(t)\{q^*(t) \otimes \boldsymbol{v}(t) \otimes q(t)\}$ represents the drag force, which is proportional to the velocity in the xy plane of the quadrotor. The x and y components of $\tilde{\boldsymbol{a}}(t)$ suggest that the acceleration measured in the horizontal plane is proportional to the velocity in the vehicle coordinate frame. Moreover, the z component of $\tilde{\boldsymbol{a}}(t)$ relates the thrust force to the acceleration in the vertical direction. Acceleration measurement is described without using gravitational acceleration.

The direction of the acceleration is also related to the attitude. Because the magnitude of the proper acceleration of a small quadrotor is not comparable to the gravitational acceleration g, the acceleration measured by the accelerometer is regarded as gravitational acceleration in the vehicle coordinate system. Thus, it points outward from the center of the earth. The direction is expressed by the unit vector of the measured acceleration. The measurement model of the acceleration direction for the attitude measurement is described below. The acceleration direction is expressed by $\boldsymbol{d}_a(t) = \begin{bmatrix} d_{a,x}(t) & d_{a,y}(t) & d_{a,z}(t) \end{bmatrix}^T$.

$$\boldsymbol{d}_a(t) \triangleq \frac{\tilde{\boldsymbol{a}}(t)}{\|\tilde{\boldsymbol{a}}(t)\|} = q^*(t) \otimes (-q_{e_3}) \otimes q(t)$$
$$= \boldsymbol{R}^T(q(t))(-\boldsymbol{e}_3), \tag{12}$$

where

$$\boldsymbol{e}_3 = \begin{bmatrix} 0 & 0 & 1 \end{bmatrix}^T \text{ and } q_{e_3} = \begin{bmatrix} 0 & \boldsymbol{e}_3 \end{bmatrix}^T.$$

The geomagnetic field at a given point on earth can be regarded as constant over a period of several days, and it can be used as a reference for the measurement of attitude.

It is primarily used as a horizontal reference of attitude, whereas the acceleration direction $\boldsymbol{d}_a(t)$ serves as an attitude reference in the vertical direction. Therefore, it is only required to use the horizontal component of the geomagnetic field measurement. This component is extracted by using the cross-product of the measured magnetic field and the vertical directional vector that is represented by gravitational acceleration. Because the direction is of interest, this cross-product vector is also normalized to obtain the direction measurement $\boldsymbol{d}_m(t)$ of the geomagnetic field as follows:

$$\boldsymbol{d}_m(t) \triangleq \frac{\tilde{\boldsymbol{m}}(t) \times \tilde{\boldsymbol{a}}(t)}{\|\tilde{\boldsymbol{m}}(t) \times \tilde{\boldsymbol{a}}(t)\|}$$
$$= q^*(t) \otimes \left\{ \frac{{}^w\boldsymbol{m} \times (-\boldsymbol{e}_3)}{\|{}^w\boldsymbol{m} \times (-\boldsymbol{e}_3)\|} \right\} \otimes q(t)$$
$$= \boldsymbol{R}^T(q(t)) \left\{ \frac{{}^w\boldsymbol{m} \times (-\boldsymbol{e}_3)}{\|{}^w\boldsymbol{m} \times (-\boldsymbol{e}_3)\|} \right\}, \qquad (13)$$

where ${}^w\boldsymbol{m} = \begin{bmatrix} {}^wm_x & {}^wm_y & {}^wm_z \end{bmatrix}^T$ is the geomagnetic field vector that can be identified by the world magnetic model at the place of navigation [31].

The angular rate $\tilde{\boldsymbol{\omega}}(t)$ and barometric altitude $\tilde{z}(t)$ are directly related to the state variables, as follows:

$$\tilde{\boldsymbol{\omega}}(t) = \boldsymbol{\omega}(t), \qquad (14)$$
$$\tilde{z}(t) = z(t). \qquad (15)$$

The measurement equation $\boldsymbol{h}(\mathbf{x}(t), \boldsymbol{u}(t))$ consists of (11), (12), (13), (14), and (15).

The proposed measurement model differs from that of [27] in excluding roll $\phi(t)$ and pitch $\theta(t)$ from the measurement vector. Instead, it includes the unit acceleration vector $\boldsymbol{d}_a(t)$ and unit horizontal component $\boldsymbol{d}_m(t)$ of the magnetic field vector. These differences allow the proposed measurement model to have the following advantages over the previous model [27]. (1) Yaw estimation performance is improved because the horizontal component of the geomagnetic field acts as a reference for yaw estimation. (2) The elements of the Jacobian matrix of the measurement model did not diverge, unlike the previous model where some components of the Jacobian diverge.

By incorporating the unit horizontal magnetic field vector $\boldsymbol{d}_m(t)$, yaw information is considered in the measurement update stage of the estimation. Because only the horizontal component of the magnetic field is used, the magnetic field vector as a measurement does not deteriorate the roll and pitch estimation. The roll and pitch are measured using the unit acceleration vector $\boldsymbol{d}_a(t)$.

By using the vectors as the measurement instead of the Euler angles, divergence of the Jacobian of the measurement model is avoided. Equation (17) of [27] indicates that pitch is represented using the inverse of the sine function as follows:

$$\theta(t) = \sin^{-1}(q_t(t)), \qquad (16)$$

where

$$q_t(t) = 2\{q_w(t) q_y(t) - q_x(t) q_z(t)\}.$$

The Jacobian matrix $\boldsymbol{H}(t)$ of the measurement model of [27] includes the partial derivatives of $\theta(t)$ with respect to the quaternion components. The partial derivatives are as follows:

$$\frac{\partial \theta(t)}{\partial q_*(t)} = \frac{1}{\sqrt{1 - q_t^2(t)}} \cdot \frac{\partial q_t(t)}{\partial q_*(t)}, \qquad (17)$$

where $* \in \{w, x, y, z\}$.

The partial derivative $\frac{\partial \theta(t)}{\partial q_*(t)}$ becomes infinite as $q_t(t)$ approaches 1 or −1, which is the case when the pitch θ approaches $\pi/2$ or $-\pi/2$. This indicates that the Jacobian $\boldsymbol{H}(t)$ of the measurement model in [27] diverges depending on the attitude of the quadrotor. By contrast, as derived in Section III-B, no component of the Jacobian of the proposed measurement model diverges.

III. USE OF LIE GROUP S^3 FOR ESTIMATION

The process and measurement models use unit quaternions that constitute a Lie group S^3 (unit 3-sphere group). Linearization of the models is required when using the EKF. The partial derivatives required for linearization can be obtained in S^3 by using the corresponding Lie algebra $\mathfrak{s}^3$. The following sections present the process for obtaining Jacobian matrices using partial derivatives in S^3. Details are provided in Appendix A.

A. JACOBIAN OF PROCESS MODEL
1) JACOBIAN MATRIX
The process equation (2) is discretized and augmented by adding the process noise $\boldsymbol{n}_s(t_i)$ to obtain the model $\boldsymbol{f}_d(\mathbf{x}(t_i), \boldsymbol{u}(t_i), \boldsymbol{n}_s(t_i))$ that fits the discrete-time KF as follows:

$$\mathbf{x}(t_{i+1}) = \boldsymbol{f}_d(\mathbf{x}(t_i), \boldsymbol{u}(t_i), \boldsymbol{n}_s(t_i)). \qquad (18)$$

The noise $\boldsymbol{n}_s(t_i)$ consists of the noise in position $\boldsymbol{n}_x(t_i)$, noise in velocity $\boldsymbol{n}_v(t_i)$, noise in attitude $\boldsymbol{n}_q(t_i)$, and noise in the angular rate $\boldsymbol{n}_\omega(t_i)$:

$$\boldsymbol{n}_s(t_i) = \begin{bmatrix} \boldsymbol{n}_x(t_i) & \boldsymbol{n}_v(t_i) & \boldsymbol{n}_q(t_i) & \boldsymbol{n}_\omega(t_i) \end{bmatrix}^T,$$
$$\boldsymbol{n}_*(t_i) \sim \mathcal{N}(0, \boldsymbol{Q}_*(t_i)), \quad * \in \{x, v, q, \omega\}. \qquad (19)$$

Each of $\boldsymbol{n}_x(t_i)$, $\boldsymbol{n}_v(t_i)$, and $\boldsymbol{n}_\omega(t_i)$ is in $\boldsymbol{R}^3$ and is assumed to be additive. In particular, the noise in attitude $\boldsymbol{n}_q(t_i)$ is additive in three-dimensional Lie algebra $\mathfrak{s}^3$. The incorporation of $\boldsymbol{n}_q(t_i)$ into the measurement equation is explained in Sections III-A3 and III-C using Lie group theory.

The Jacobian matrix for the discretized process model (18) is as follows.

$$\boldsymbol{F}(t_{i+1})$$

$$= \begin{bmatrix} \dfrac{\partial \boldsymbol{x}(t_{i+1})}{\partial \boldsymbol{x}(t_i)} & \dfrac{\partial \boldsymbol{x}(t_{i+1})}{\partial \boldsymbol{v}(t_i)} & \dfrac{\partial \boldsymbol{x}(t_{i+1})}{\partial q(t_i)} & \dfrac{\partial \boldsymbol{x}(t_{i+1})}{\partial \boldsymbol{\omega}(t_i)} \\[1em] \dfrac{\partial \boldsymbol{v}(t_{i+1})}{\partial \boldsymbol{x}(t_i)} & \dfrac{\partial \boldsymbol{v}(t_{i+1})}{\partial \boldsymbol{v}(t_i)} & \dfrac{\partial \boldsymbol{v}(t_{i+1})}{\partial q(t_i)} & \dfrac{\partial \boldsymbol{v}(t_{i+1})}{\partial \boldsymbol{\omega}(t_i)} \\[1em] \dfrac{\partial q(t_{i+1})}{\partial \boldsymbol{x}(t_i)} & \dfrac{\partial q(t_{i+1})}{\partial \boldsymbol{v}(t_i)} & \dfrac{\partial q(t_{i+1})}{\partial q(t_i)} & \dfrac{\partial q(t_{i+1})}{\partial \boldsymbol{\omega}(t_i)} \\[1em] \dfrac{\partial \boldsymbol{\omega}(t_{i+1})}{\partial \boldsymbol{x}(t_i)} & \dfrac{\partial \boldsymbol{\omega}(t_{i+1})}{\partial \boldsymbol{v}(t_i)} & \dfrac{\partial \boldsymbol{\omega}(t_{i+1})}{\partial q(t_i)} & \dfrac{\partial \boldsymbol{\omega}(t_{i+1})}{\partial \boldsymbol{\omega}(t_i)} \end{bmatrix}$$

$$= \begin{bmatrix} \mathbf{I}_3 & \Delta t_{i+1}\mathbf{I}_3 & \mathbf{0}_3 & \mathbf{0}_3 \\ \mathbf{0}_3 & \frac{\partial \mathbf{v}(t_{i+1})}{\partial \mathbf{v}(t_i)} & \frac{\partial \mathbf{v}(t_{i+1})}{\partial \mathbf{q}(t_i)} & \mathbf{0}_3 \\ \mathbf{0}_3 & \mathbf{0}_3 & \frac{\partial \mathbf{q}(t_{i+1})}{\partial \mathbf{q}(t_i)} & \frac{\partial \mathbf{q}(t_{i+1})}{\partial \boldsymbol{\omega}(t_i)} \\ \mathbf{0}_3 & \mathbf{0}_3 & \mathbf{0}_3 & \frac{\partial \boldsymbol{\omega}(t_{i+1})}{\partial \boldsymbol{\omega}(t_i)} \end{bmatrix}. \quad (20)$$

2) PARTIAL DERIVATIVES FOR VELOCITY PROPAGATION

The velocity $\mathbf{v}(t_i)$ propagates to $\mathbf{v}(t_{i+1})$ owing to the acceleration $\dot{\mathbf{v}}(t_{i+1})$ as follows:

$$\mathbf{v}(t_{i+1}) = \mathbf{v}(t_i) + \dot{\mathbf{v}}(t_i)\Delta t_{i+1} + \mathbf{n}_v(t_i)$$

$$= \mathbf{v}(t_i) + \begin{bmatrix} 0 \\ 0 \\ g \end{bmatrix} \Delta t_{i+1} + \mathbf{R}(q(t_i))\mathbf{a}_r(t_i)\Delta t_{i+1}$$

$$+ \mathbf{R}(q(t_i)) \left\{ \mathbf{V}(t_i)\mathbf{R}^T(q(t_i))\mathbf{v}(t_i) \right\} \Delta t_{i+1}$$

$$+ \mathbf{n}_v(t_i). \quad (21)$$

In the description of the partial derivatives, the following shorthand notations are used for simplicity:

$$\mathbf{R} = \mathbf{R}(q(t_i)),$$
$$\mathbf{V} = \mathbf{V}(t_i),$$
$$\mathbf{v} = \mathbf{v}(t_i),$$
$$\mathbf{a}_r = \mathbf{a}_r(t_i),$$
$$\Delta t = \Delta t_{i+1}.$$

First, the partial derivative of $\mathbf{v}(t_{i+1})$ with respect to $\mathbf{v}(t_i)$ is obtained as follows:

$$\frac{\partial \mathbf{v}(t_{i+1})}{\partial \mathbf{v}(t_i)} = \mathbf{I}_3 + \mathbf{R}\mathbf{V}\mathbf{R}^T \Delta t. \quad (22)$$

The partial derivative of $\mathbf{v}(t_{i+1})$ with respect to $q(t_i)$ is obtained as follows:

$$\frac{\partial \mathbf{v}(t_{i+1})}{\partial \mathbf{q}(t_i)} = -\mathbf{R} \left\{ [\mathbf{a}_r]_\times + \left[\mathbf{V}\mathbf{R}^T \mathbf{v} \right]_\times - \mathbf{V} \left[\mathbf{R}^T \mathbf{v} \right]_\times \right\} \Delta t. \quad (23)$$

The partial derivatives of $\mathbf{v}(t_{i+1})$ with respect to $\mathbf{x}(t_i)$ and $\boldsymbol{\omega}(t_i)$ are both zero:

$$\frac{\partial \mathbf{v}(t_{i+1})}{\partial \mathbf{x}(t_i)} = \frac{\partial \mathbf{v}(t_{i+1})}{\partial \boldsymbol{\omega}(t_i)} = \mathbf{0}_3. \quad (24)$$

3) PARTIAL DERIVATIVES FOR ATTITUDE PROPAGATION

Using Lie group theory and (7), attitude propagation from $q(t_i)$ to $q(t_{i+1})$ can be expressed as follows:

$$q(t_{i+1}) = q(t_i) \otimes \text{Exp}(\boldsymbol{\omega}(t_i)\Delta t_{i+1}) \otimes \text{Exp}(\mathbf{n}_q(t_i)), \quad (25)$$

where $\mathbf{n}_q(t_i) \in \mathbf{R}^3$ is the noise vector in the attitude propagation represented by the unit quaternions in S^3. In (25), the function $\text{Exp}(\cdot)$ is the exponential map, which maps a vector in $\mathbf{R}^3$ to an element in S^3 as follows [20]:

$$\text{Exp}(\mathbf{p}) = \begin{bmatrix} \cos\left(\frac{\|\mathbf{p}\|}{2}\right) \\ \frac{\mathbf{p}}{\|\mathbf{p}\|} \sin\left(\frac{\|\mathbf{p}\|}{2}\right) \end{bmatrix}, \quad (26)$$

where $\mathbf{p}$ is the vector equivalent of an element in Lie algebra $\mathfrak{s}^3$. Although (25) expresses attitude propagation as quaternion multiplication in space S^3, quaternion multiplication corresponds to addition in Lie algebra $\mathfrak{s}^3$. Therefore, the noise $\mathbf{n}_q(t_i)$ is additive in $\mathfrak{s}^3$. The partial derivatives are obtained under the condition $\mathbf{n}_q(t_i) = \mathbf{0}$.

The partial derivative of $q(t_{i+1})$ with respect to $q(t_i)$ is:

$$\frac{\partial q(t_{i+1})}{\partial q(t_i)} = \mathbf{R}^T(\boldsymbol{\omega}\Delta t), \quad (27)$$

where $\mathbf{R}^T(\boldsymbol{\omega}\Delta t)$ denotes the rotation matrix corresponding to the rotation vector $\mathbf{r} = \boldsymbol{\omega}\Delta t = \boldsymbol{\omega}(t_i)\Delta t_{i+1}$ as follows:

$$\mathbf{R}(\mathbf{r}) = \mathbf{I}_3 + \sin(\|\mathbf{r}\|) \left[\frac{\mathbf{r}}{\|\mathbf{r}\|} \right]_\times + (1 - \cos(\|\mathbf{r}\|)) \left[\frac{\mathbf{r}}{\|\mathbf{r}\|} \right]_\times^2. \quad (28)$$

The partial derivative of $q(t_{i+1})$ with respect to $\boldsymbol{\omega}(t_i)$ is

$$\frac{\partial q(t_{i+1})}{\partial \boldsymbol{\omega}(t_i)} = \left(\mathbf{I}_3 - \frac{1 - \cos\|\mathbf{r}\|}{\|\mathbf{r}\|^2} [\mathbf{r}]_\times \right.$$

$$\left. + \frac{\|\mathbf{r}\| - \sin\|\mathbf{r}\|}{\|\mathbf{r}\|^3} [\mathbf{r}]_\times^2 \right) \Delta t. \quad (29)$$

The partial derivatives of $q(t_{i+1})$ with respect to $\mathbf{x}(t_i)$ and $\mathbf{v}(t_i)$ are both zero:

$$\frac{\partial q(t_{i+1})}{\partial \mathbf{x}(t_i)} = \frac{\partial q(t_{i+1})}{\partial \mathbf{v}(t_i)} = \mathbf{0}_3. \quad (30)$$

4) PARTIAL DERIVATIVES FOR ANGULAR RATE PROPAGATION

The partial derivative of angular rate $\boldsymbol{\omega}(t_{i+1})$ with respect to $\boldsymbol{\omega}(t_i)$ is

$$\frac{\partial \boldsymbol{\omega}(t_{i+1})}{\partial \boldsymbol{\omega}(t_i)} = \mathbf{I}_3 + \begin{bmatrix} 0 & w_{1,2} & w_{1,3} \\ w_{2,1} & 0 & w_{2,3} \\ w_{3,1} & w_{3,2} & 0 \end{bmatrix} \Delta t, \quad (31)$$

where

$$w_{1,2} = \frac{I_{yy} - I_{zz}}{I_{xx}} a_z, \quad w_{1,3} = \frac{I_{yy} - I_{zz}}{I_{xx}} a_y,$$

$$w_{2,1} = \frac{I_{zz} - I_{xx}}{I_{yy}} a_z, \quad w_{2,3} = \frac{I_{zz} - I_{xx}}{I_{yy}} a_x,$$

$$w_{3,1} = \frac{I_{xx} - I_{yy}}{I_{zz}} a_y, \quad w_{3,2} = \frac{I_{xx} - I_{yy}}{I_{zz}} a_x.$$

B. JACOBIAN OF MEASUREMENT MODEL
1) JACOBIAN MATRIX

The Jacobian matrix of the measurement model $\mathbf{z}(t) = \mathbf{h}(\mathbf{x}(t), \mathbf{u}(t)) + \mathbf{n}_m(t)$ is partitioned according to the partial derivatives of the measurements with respect to the states,

as follows:

$$
H(t_i) =
\begin{bmatrix}
\dfrac{\partial \tilde{a}(t_i)}{\partial x(t_i)} & \dfrac{\partial \tilde{a}(t_i)}{\partial v(t_i)} & \dfrac{\partial \tilde{a}(t_i)}{\partial q(t_i)} & \dfrac{\partial \tilde{a}(t_i)}{\partial \omega(t_i)} \\[2mm]
\dfrac{\partial d_a(t_i)}{\partial x(t_i)} & \dfrac{\partial d_a(t_i)}{\partial v(t_i)} & \dfrac{\partial d_a(t_i)}{\partial q(t_i)} & \dfrac{\partial d_a(t_i)}{\partial \omega(t_i)} \\[2mm]
\dfrac{\partial d_m(t_i)}{\partial x(t_i)} & \dfrac{\partial d_m(t_i)}{\partial v(t_i)} & \dfrac{\partial d_m(t_i)}{\partial q(t_i)} & \dfrac{\partial d_m(t_i)}{\partial \omega(t_i)} \\[2mm]
\dfrac{\partial \tilde{\omega}(t_i)}{\partial x(t_i)} & \dfrac{\partial \tilde{\omega}(t_i)}{\partial v(t_i)} & \dfrac{\partial \tilde{\omega}(t_i)}{\partial q(t_i)} & \dfrac{\partial \tilde{\omega}(t_i)}{\partial \omega(t_i)} \\[2mm]
\dfrac{\partial \tilde{z}(t_i)}{\partial x(t_i)} & \dfrac{\partial \tilde{z}(t_i)}{\partial v(t_i)} & \dfrac{\partial \tilde{z}(t_i)}{\partial q(t_i)} & \dfrac{\partial \tilde{z}(t_i)}{\partial \omega(t_i)}
\end{bmatrix}
$$

$$
=
\begin{bmatrix}
\mathbf{0}_3 & \dfrac{\partial \tilde{a}(t_i)}{\partial v(t_i)} & \dfrac{\partial \tilde{a}(t_i)}{\partial q(t_i)} & \mathbf{0}_3 \\[2mm]
\mathbf{0}_3 & \mathbf{0}_3 & \dfrac{\partial d_a(t_i)}{\partial q(t_i)} & \mathbf{0}_3 \\[2mm]
\mathbf{0}_3 & \mathbf{0}_3 & \dfrac{\partial d_m(t_i)}{\partial q(t_i)} & \mathbf{0}_3 \\[2mm]
\mathbf{0}_3 & \mathbf{0}_3 & \mathbf{0}_3 & I_3 \\[2mm]
\begin{bmatrix}0 & 0 & 1\end{bmatrix} & \mathbf{0}_{1\times 3} & \mathbf{0}_{1\times 3} & \mathbf{0}_{1\times 3}
\end{bmatrix}.
\tag{32}
$$

Each partial derivative of the measurements with respect to a quaternion has three columns, even though a unit quaternion in S^3 has four components, because the increments of the unit quaternions constitute the tangent space $\mathfrak{s}^3$, which is three-dimensional. Therefore, the partial derivatives of the measurements with respect to the unit quaternions are obtained using the theory of Lie groups and Lie algebras in the following sections.

2) PARTIAL DERIVATIVES OF ACCELERATION MEASUREMENT

The partial derivatives of the acceleration measurement with respect to the states are obtained from (11), as follows:

$$
\frac{\partial \tilde{a}(t_i)}{\partial v(t_i)} = \Lambda(t_i) R^T(q(t_i)),
\tag{33}
$$

$$
\frac{\partial \tilde{a}(t_i)}{\partial q(t_i)} = \Lambda(t_i) \left[R^T(q(t_i)) v(t_i) \right]_\times ,
\tag{34}
$$

$$
\frac{\partial \tilde{a}(t_i)}{\partial x(t_i)} = \frac{\partial \tilde{a}(t_i)}{\partial \omega(t_i)} = \mathbf{0}_3.
\tag{35}
$$

3) PARTIAL DERIVATIVES OF ACCELERATION DIRECTION

The partial derivatives of the acceleration direction with respect to the states are obtained from (12) as follows:

$$
\frac{\partial d_a(t_i)}{\partial q(t_i)} = \left[R^T(q(t_i))(-e_3) \right]_\times ,
\tag{36}
$$

$$
\frac{\partial d_a(t_i)}{\partial x(t_i)} = \frac{\partial d_a(t_i)}{\partial v(t_i)} = \frac{\partial d_a(t_i)}{\partial \omega(t_i)} = \mathbf{0}_3.
\tag{37}
$$

4) PARTIAL DERIVATIVES OF GEOMAGNETIC FIELD DIRECTION

The partial derivatives of the geomagnetic field direction with respect to the states are obtained from (13), as follows:

$$
\frac{\partial d_m(t_i)}{\partial q(t_i)} = \left[R^T(q(t_i)) \left\{ \frac{{}^w m \times (-e_3)}{\| {}^w m \times (-e_3) \|} \right\} \right]_\times
$$
$$
= \left[R^T(q(t_i)) \left\{ \frac{e_3 \times {}^w m}{\| e_3 \times {}^w m \|} \right\} \right]_\times ,
\tag{38}
$$

$$
\frac{\partial d_m(t_i)}{\partial x(t_i)} = \frac{\partial d_m(t_i)}{\partial v(t_i)} = \frac{\partial d_m(t_i)}{\partial \omega(t_i)} = \mathbf{0}_3.
\tag{39}
$$

C. EKF PROCEDURE

The state estimation is implemented using EKF. The EKF uses the Jacobian matrices derived in Sections III-A and III-B. In addition to using the Jacobian matrices derived in Lie group and Lie algebra, the EKF uses operations in Lie group and Lie algebra to evaluate the attitude.

The attitude is propagated using the exponential of the vector $\omega(t_i)\Delta t_{i+1}$, which is the angular increment during Δt_{i+1}, and the vector counterpart of the increment in Lie algebra $\mathfrak{s}^3$. Therefore, attitude propagation is represented using the following equation:

$$
\hat{q}(t_{i+1}^-) = \hat{q}(t_i) \otimes \mathrm{Exp}(\omega(t_i)\Delta t_{i+1}),
\tag{40}
$$

where $\hat{q}(t_{i+1}^-)$ is the state at time t_{i+1} propagated from the previously estimated state $\hat{q}(t_i)$ at time t_i. The use of the exponential ensures accurate predictions and preserves the norm of the predicted unit quaternion. On the contrary, numerical integration of (7) results in approximated predictions and does not satisfy the unit norm constraint.

The process noise covariance $Q_s(t)$, which appears in process models (18) and (19), requires further analysis. In (25), $n_q(t_i)$ is a vector describing the difference between the two unit quaternions in S^3, which belongs to Lie algebra $\mathfrak{s}^3$, the tangent space of S^3. The addition of elements in $\mathfrak{s}^3$ and scalar multiplication of $\mathfrak{s}^3$ elements results in elements in $\mathfrak{s}^3$. The error covariance for $\hat{q}(t_{i+1}^-)$ is of dimension 3×3 as shown below:

$$
P_{\hat{q}\hat{q}}(t_{i+1}^-) = E\left[e_{\hat{q}}(t_{i+1}^-) e_{\hat{q}}(t_{i+1}^-)^T \right],
\tag{41}
$$

where $e_{\hat{q}}(t_{i+1}^-)$ is the difference between the prediction $\hat{q}(t_{i+1}^-)$ and $q(t_{i+1})$ obtained as follows:

$$
e_{\hat{q}}(t_{i+1}^-) = \left(q^{-1}(t_{i+1}) \otimes \hat{q}(t_{i+1}^-) \right)^\vee .
\tag{42}
$$

In (42), $\left(q^{-1}(t_{i+1}) \otimes \hat{q}(t_{i+1}^-) \right)$ is in $\mathfrak{s}^3$, and operator $(\cdot)^\vee$ maps a Lie algebra element in $\mathfrak{s}^3$ to the corresponding vector in R^3. Thus, the predicted state $\hat{x}(t_{i+1}^-)$ has an error covariance matrix of dimension 12×12. This is one of the distinct features of Lie group implementation of the EKF compared to the implementation of the EKF in [27], where $\hat{x}(t_{i+1}^-)$ has an error covariance matrix of dimension 13×13. The method in [27] considered a unit quaternion as a variable in R^4 instead of S^3. The addition and scalar multiplication of vectors in R^4 do not result in elements in S^3.

The measurement update stage of the EKF adds the correction state $\delta\mathbf{x}(t_{i+1})$ to the predicted state $\hat{\mathbf{x}}(t_{i+1}^{-})$ as follows:

$$\hat{\mathbf{x}}(t_{i+1}) = \hat{\mathbf{x}}(t_{i+1}^{-}) + \delta\mathbf{x}(t_{i+1}), \qquad (43)$$

where

$$
\begin{aligned}
\delta\mathbf{x}(t_{i+1}) &= [\delta\boldsymbol{x}(t_{i+1})\ \ \delta\boldsymbol{v}(t_{i+1})\ \ \delta q(t_{i+1})\ \ \delta\boldsymbol{\omega}(t_{i+1})]^{T} \\
&= \boldsymbol{K}(t_{i+1})\left\{z(t_{i+1}) - \boldsymbol{h}(\hat{\mathbf{x}}(t_{i+1}^{-}), \boldsymbol{u}(t_{i+1}))\right\}.
\end{aligned}
$$

The correction state $\delta\mathbf{x}(t_{i+1})$ is the Kalman gain $\boldsymbol{K}(t_{i+1})$ multiplied by the measurement innovation at time $t = t_{i+1}$. The vector $\delta q(t_{i+1})$, which is used for the attitude measurement update, is a subvector of $\delta\mathbf{x}(t_{i+1})$:

$$\delta q(t_{i+1}) = \delta\mathbf{x}(t_{i+1})(7:9), \qquad (44)$$

where $\delta\mathbf{x}(t_{i+1})(7:9)$ denotes the subvector of $\delta\mathbf{x}(t_{i+1})$; the elements of the subvector are the seventh to ninth elements of $\delta\mathbf{x}(t_{i+1})$.

The correction state $\delta\mathbf{x}(t_{i+1})$ has 12 elements; however, the predicted state $\hat{\mathbf{x}}(t_{i+1}^{-})$ has 13 elements. The attitude correction $\delta q(t_{i+1})$ has three elements belonging to Lie algebra $\mathfrak{s}^3$. Therefore, adding $\delta q(t_{i+1})$ to the predicted attitude $\hat{q}(t_{i+1}^{-})$ is not a meaningful operation, and Lie theory is required to append $\delta q(t_{i+1})$ to $\hat{q}(t_{i+1}^{-})$. Lie theory is applied in the measurement update to multiply the predicted attitude $\hat{q}(t_{i+1}^{-})$ by the exponential of the correction state $\delta q(t_{i+1})$ as follows:

$$\hat{q}(t_{i+1}) = \hat{q}(t_{i+1}^{-}) \otimes \mathrm{Exp}(\delta q(t_{i+1})). \qquad (45)$$

The measurement update using (45) is exact. In an EKF where the quaternion $\hat{q}(t_{i+1}^{-})$ and the correction vector are treated as vectors in $\boldsymbol{R}^4$, the correction vector is added to $\hat{q}(t_{i+1}^{-})$ in the measurement update procedure. However, in vector addition, the geometrical properties of the attitude are not considered; furthermore, vector addition provides an approximated update that does not constrain the norm of the updated quaternion to 1 [27]. Therefore, approximation errors are inevitable, and normalization is required.

IV. EXPERIMENTS AND RESULTS

The improvement owing to the proposed method is verified experimentally in this section. For comparison, the experiments were conducted using the same quadrotor and sensor set as in [27]. Details of the quadrotor and sensors are provided in [27]. The method was tested on two flight datasets: one dataset was the same as that used in [27] and the other was a new dataset with a different trajectory. The first dataset was collected from a level flight and was termed Flight Test 1. The quadrotor flew approximately 190 m in 45 s at an altitude of 8.5 m without an altitude change. In the second dataset, the quadrotor traversed the trajectory twice through a round-trip path. The altitude varied by 10 m during the flight. The quadrotor flew approximately 449 m in 124 s while varying the altitude between 8 m and 18 m. The second experiment was termed Flight Test 2.

As the feasibility and performance of DMAN were demonstrated in [27], the present study primarily focused on the
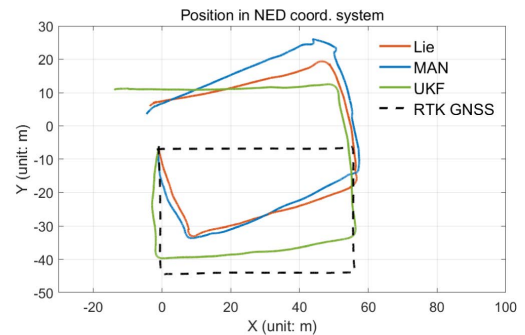
(a) Estimated trajectories in Flight Test 1
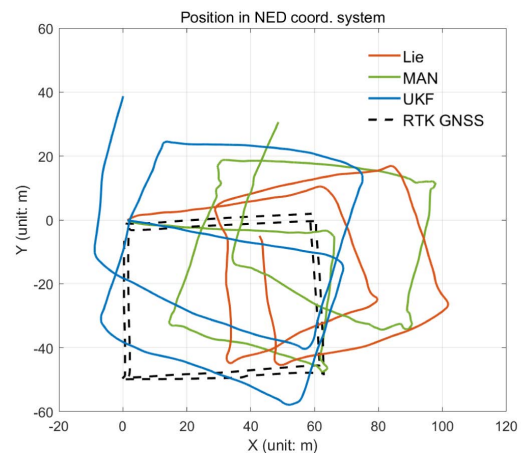
(b) Estimated trajectories in Flight Test 2

FIGURE 2. Comparison of estimated trajectories.

advantage of applying Lie group theory to DMAN. The comparison with the previous DMAN focuses on two aspects: estimation and properties of internal variables. Estimation refers to the estimated location, attitude, and velocity. The internal variables refer to the measurement innovation and Kalman gain. Hereafter, in the figures and tables, the proposed approach is referenced as "Lie," whereas "MAN" and "UKF" refer to the previous approaches [27] which use EKF and UKF respectively.

Figure 2 shows the estimated trajectories in the *xy* plane for both experiments. As exteroceptive measurements are not used in the estimation process, shifts and tilts are inevitable in the estimated trajectory, and the estimation error accumulates with time and travel distance. The location and attitude relative to the initial location and attitude are thus more significant than the absolute location and attitude. Therefore, the error in the trajectory estimation was calculated using the estimated trajectory, which was rotated and shifted to fit the true trajectory as closely as possible. The translation and rotation for the trajectory fitting were determined using the nonlinear least-squares method [32].

Figure 3 shows the estimated *x*-directional velocity and yaw for Flight Test 2. The results indicated that the estimated velocity and attitude allowed dead reckoning for a short time; however, the trajectory deviation increased with time and travel distance.
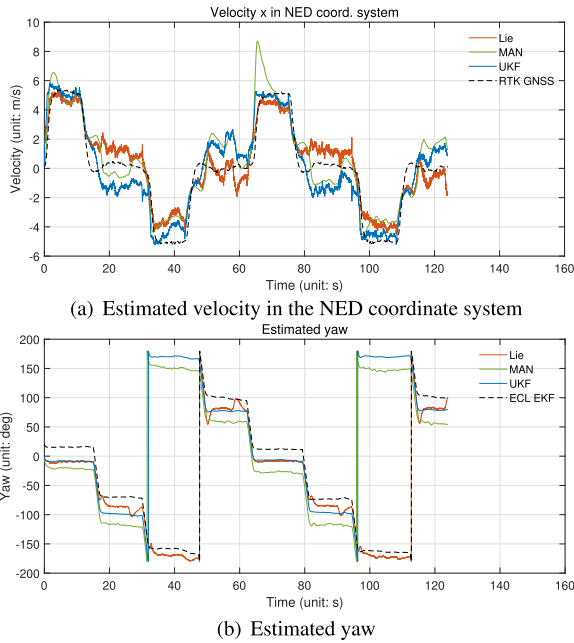
(a) Estimated velocity in the NED coordinate system

(b) Estimated yaw

FIGURE 3. Estimated x-directional velocity and yaw in Flight Test 2.

TABLE 1. Root mean square distance error of the estimated locations (m).

	Flight Test 1			Flight Test 2		
	Lie	MAN	UKF	Lie	MAN	UKF
RMSE	3.5134	4.0471	5.9435	12.278	18.374	14.419

Lie: Proposed Lie-group-based method
MAN: EKF Method in [27]
UKF: UKF Method in [27]

TABLE 2. Error analysis of the velocity estimated in the vehicle coordinate frame (m/s).

Stat	Di.	Flight Test 1			Flight Test 2		
		Lie	MAN	UKF	Lie	MAN	UKF
Mn	x	-0.1273	0.1232	0.0660	-0.1920	0.0525	0.7430
	y	-1.0944	-1.3348	-0.1788	-0.0683	-0.2443	1.3852
	z	-0.0873	-1.1568	-0.1579	1.0448	1.1332	2.4022
Std	x	1.5961	1.6151	0.6651	1.0346	1.1198	0.7613
	y	0.9376	0.9722	0.6966	0.5742	0.7436	0.6422
	z	2.9611	1.3239	0.8184	1.7331	2.1894	3.2213
RMSE	x	1.6011	1.6198	0.6683	1.0523	1.1211	1.0638
	y	1.4411	1.6513	0.7192	0.5783	0.7827	1.5268
	z	2.9624	1.7581	0.8335	2.0237	2.4653	4.0183

Stat: Statistic
Di.: Direction
Mn: Mean of the error
Std: Standard deviation of the error

TABLE 3. Error analysis of the estimated attitude (degrees).

Stat	At.	Flight Test 1			Flight Test 2		
		Lie	MAN	UKF	Lie	MAN	UKF
Mn	ϕ	-1.4553	-3.0653	-0.4103	0.5039	0.8263	-0.4847
	θ	-0.4240	15.4068	1.0184	-2.8695	-4.9285	-0.8653
	ψ	-1.7876	0.5099	3.5377	-15.4993	-43.0392	-29.0480
Std	ϕ	3.0367	3.9133	1.6108	1.0518	1.6904	2.5469
	θ	6.5890	3.2258	1.2520	6.5242	2.7753	2.4698
	ψ	26.6368	27.2843	3.0892	8.6150	5.2527	5.8414
RMSE	ϕ	3.3688	4.9705	1.6623	1.1663	1.8815	2.5926
	θ	6.6022	15.7401	1.6138	7.1273	5.6562	2.6170
	ψ	26.6982	27.2900	4.6966	17.7326	43.3586	29.6296

At.: Attitude
ϕ: Roll, θ: Pitch, ψ: Yaw

A comparison of the errors in location estimation is presented in Table 1. The position error is the distance between the estimated and reference locations. The location detected by the real-time kinematic GNSS was regarded as the reference location for the error calculation. For both tests, the Lie-group-based approach estimated the trajectory more accurately than the previous approaches. The quadrotor flew for a longer distance and time at varying altitudes in Flight Test 2 compared with Flight Test 1. Therefore, the root-mean-square error (RMSE) for Flight Test 2 was larger than that for Flight Test 1. Moreover, the RMSE difference for the approaches increased as the travel distance increased and altitude changed.

A comparison of the errors in the estimated velocity calculated in the vehicle coordinate frame is provided in Table 2, and the corresponding comparison for the estimated attitude is provided in Table 3. The attitude estimated using the Estimation and Control Library EKF (ECL EKF) was used as a reference for the error calculation because it is regarded as the closest estimation of the true attitude, as the ECL EKF uses all sensor measurements including GNSS information [33].

The velocity and attitude errors are graphically compared in Figures 4 and 5 based on the data presented in Tables 2 and 3. The proposed method resulted in a smaller error than the previous methods [27] for most of the estimation components in Flight Test 2. The smaller mean error, standard deviation, and RMSE values indicate that the proposed method performed better than previous methods. In most cases, the mean error of the Lie group approach is less than or comparable to that of previous methods.

Magnetic field measurements reduced the yaw estimation drift, as shown in Figure 5. In both experiments, the drift in the yaw estimation is larger than that in the other angles. A comparison of Figure 5(a) and 5(b) shows that as the flight range increases, the drift in yaw estimation increases, whereas the drift in roll and pitch does not. In particular, in the longer flight range experiment (Flight Test 2), the Lie group-based method generates the smallest drift in yaw estimation. RMSE and mean of the yaw estimation error for the Lie group approach is the smallest among the three approaches. Because geomagnetic field measurements are vulnerable to external and internal disturbances, the drift in yaw estimation is still larger than that of roll and pitch, even when geomagnetic field measurements are used.

Figure 6 shows the Kalman gains of Flight Test 2, regarding the correction of the location and velocity estimations with respect to the measurement innovation on the angular rate around the x axis. In all cases, the Kalman gains of the Lie group approach converged faster and fluctuated less than those of the previous approaches.
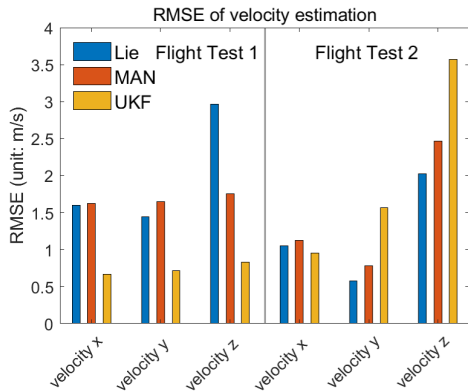
Figure 7 shows the measurement innovations for acceleration and height of Flight Test 2. Similar to the case of
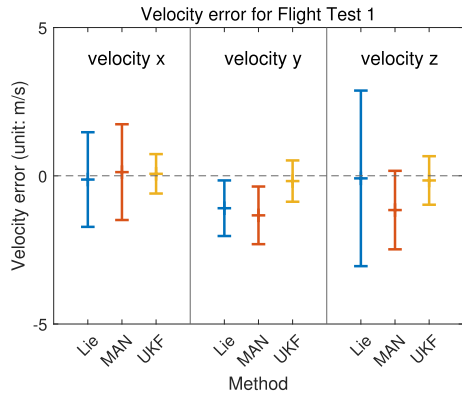
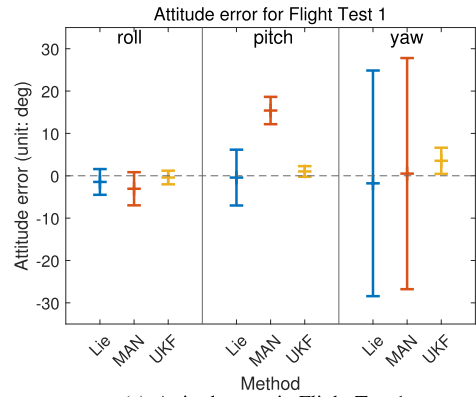(a) Velocity error in Flight Test 1
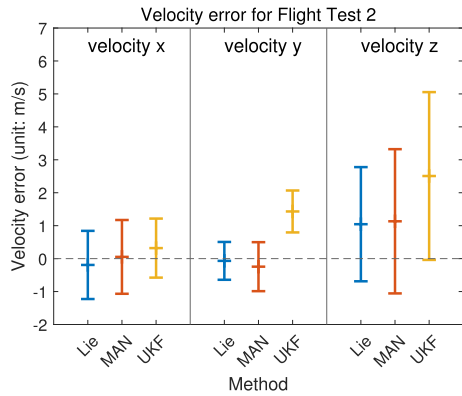
(b) Velocity error in Flight Test 2
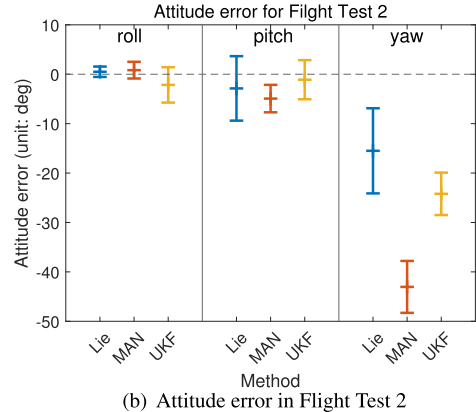
(c) RMSE of velocity estimation in Flight Test 1 and 2

FIGURE 4. Comparison of errors in velocity estimation.

(a) Attitude error in Flight Test 1

(b) Attitude error in Flight Test 2
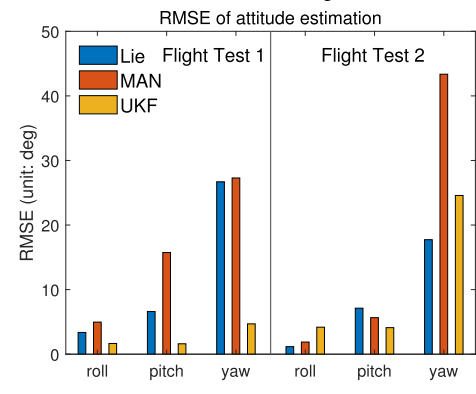
(c) RMSE of attitude estimation in Flight Test 1 and 2

FIGURE 5. Comparison of errors in attitude estimation.

Kalman gains, the measurement innovations of the Lie group approach fluctuated less, and were smaller than those of the previous approaches.

The computation time of the Lie group-based method was compared with that of the previous approaches. Because Lie and MAN use EKF, they use the same computational procedure. Compared to MAN, the Lie group-based method requires additional computation: computation of the exponential of the Lie algebra element for state prediction and state correction. The computation times of these methods are compared in Table 4. All methods were tested using MATLAB R2021a running on Windows 10 Education on a computer with an Intel(R) Core(TM) i7-10700F CPU and 16 GB

RAM running at 2.90GHz. For both datasets, the algorithms were executed 100 times. The computation times for 100 iterations were averaged. Table 4 shows that the Lie group-based method required 11–14% more time than MAN. Although the Lie group-based method requires more computation time than MAN, it still exhibits a computation time that is feasible for real-time applications.

The computational complexity of the UKF approach is the highest among the three methods. Compared to the other methods, the UKF approach requires additional computations. Cholesky decomposition of the error covariance matrix and calculation of sigma points are required. In addition, a time update is required for each sigma point. The calculation
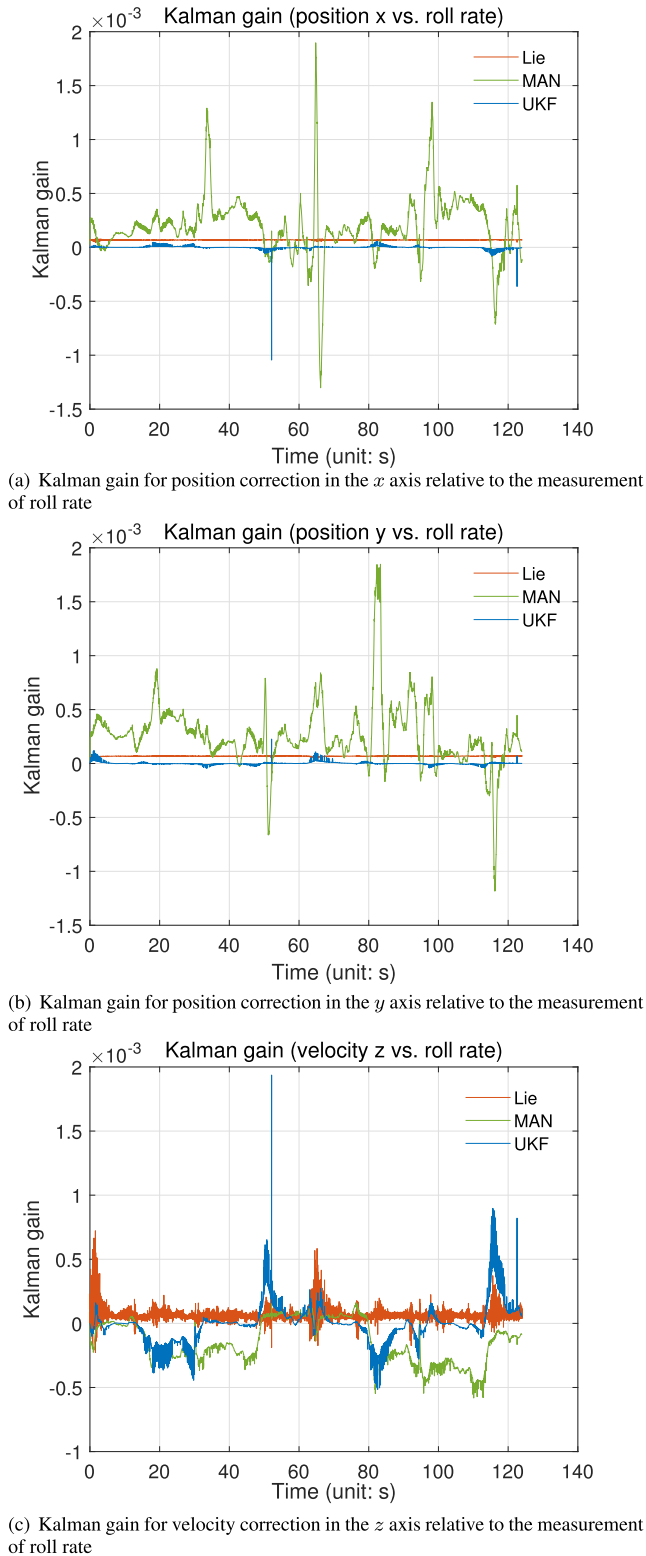
(a) Kalman gain for position correction in the x axis relative to the measurement of roll rate

(b) Kalman gain for position correction in the y axis relative to the measurement of roll rate

(c) Kalman gain for velocity correction in the z axis relative to the measurement of roll rate

FIGURE 6. Comparison of Kalman gains in the Flight Test 2.

(a) Measurement innovation of acceleration in the x direction

(b) Measurement innovation of height

FIGURE 7. Comparison of measurement innovation in Flight Test 2.

TABLE 4. Comparison of computation time.

	Flight Test 1			Flight Test 2		
	Lie	MAN	UKF	Lie	MAN	UKF
Computation time (10^{-4} s)	1.482	1.331	48.53	1.470	1.293	48.72

of covariance matrices of states and measurements involves the weighted sum of the variables of the sigma points. The cross covariance between states and measurements also requires a weighted sum. Calculation of the time update,

covariance, and cross covariance involves calculation of the sum and difference between sigma points. To obtain the sum and difference, exponential and logarithm calculations with respect to the unit quaternion are required. Accordingly, the computation time for UKF was over 30 times longer than that of the others, as shown in Table 4.

No one method outperforms the others in all aspects and for all experiments. The Lie group-based method proposed in this paper exhibited the best performance in the longer travel distance experiment, whereas UKF performed best in the experiment with a shorter travel distance. The standard deviation of the UKF approach was small. However, in the longer travel distance experiment, the Lie group-based

method outperformed the other two methods in all aspects. The advantage of the Lie group approach over the MAN and UKF approaches is evident for experiments in which the quadrotor flies longer.

The above analysis of the estimation error and the internal parameters suggests that the improvement by the Lie group approach over the previous approaches is similar to that by the invariant KF over conventional KFs, as demonstrated in [10], [11], and [34]. The estimation results were better or comparable, and the properties of the internal parameters improved significantly.

V. CONCLUSION

In this study, a Lie-group-based navigation approach for a quadrotor was proposed. Specifically, Lie group theory was utilized for the implementation of the KF, and a dynamic model was incorporated into the process and measurement models using Lie group theory. Attitude and rotation propagation were evaluated and corrected using Lie algebra and an exponential operation. Moreover, the error covariance of the attitude and rotation was properly represented. Thus, the proposed method improved the estimation results and properties of the internal parameters, namely, the Kalman gain and measurement innovation. The improvements gained by the Lie group approach were experimentally validated.

In future work, we intend to apply the Lie-group-based DMAN to underwater vehicle navigation, where hydrodynamic effects such as added mass and damping critically influence the motion of the vehicle. The application of DMAN to underwater vehicles is of practical importance because these vehicles suffer from frequent lack, delay, and distortion of ultrasonic sensor measurements, on which they depend for navigation. Accordingly, DMAN can aid navigation in the case of a lack or failure of ultrasonic sensor measurements.

APPENDIX A
DERIVATION OF PARTIAL DERIVATIVES
A. PARTIAL DERIVATIVES OF VELOCITY

The velocity at time t_{i+1} can be obtained by discretizing (4) as follows:

$$
\begin{aligned}
v(t_{i+1}) &= v(t_i) + \begin{bmatrix} 0 \\ 0 \\ g \end{bmatrix} \Delta t_{i+1} + R(q(t_i))a_r(t_i)\Delta t_{i+1} \\
&\quad + R(q(t_i))\left\{ V(t_i)R^T(q(t_i))v(t_i) \right\} \Delta t_{i+1} \\
&= v + \begin{bmatrix} 0 \\ 0 \\ g \end{bmatrix} \Delta t + Ra_r \Delta t + R\left\{ VR^T v \right\} \Delta t.
\end{aligned}
$$
(46)

Partial derivatives of $\begin{bmatrix} 0 & 0 & g \end{bmatrix}^T \Delta t_{i+1}$ and $R(q(t_i))a_r(t_i)\Delta t_{i+1}$ with respect to $v(t_i)$ are zero. The partial derivative of

$R(q(t_i))\left\{ V(t_i)R^T(q(t_i))v(t_i) \right\} \Delta t_{i+1}$ with respect to $v(t_i)$ is

$$
\begin{aligned}
\frac{\partial}{\partial v(t_i)} & R(q(t_i))\left\{ V(t_i)R^T(q(t_i))v(t_i) \right\} \Delta t_{i+1} \\
&= R(q(t_i))V(t_i)R^T(q(t_i))\Delta t_{i+1}.
\end{aligned}
$$
(47)

Therefore, $\frac{\partial v(t_{i+1})}{\partial v(t_i)}$ is

$$
\frac{\partial v(t_{i+1})}{\partial v(t_i)} = I_3 + RVR^T \Delta t.
$$
(48)

In (46), the partial derivatives of $v(t_i)$ and $\begin{bmatrix} 0 & 0 & g \end{bmatrix}^T \Delta t_{i+1}$ with respect to $q(t_i)$ are zero. The partial derivative of $R(q(t_i))a_r(t_i)\Delta t_{i+1}$ with respect to $q(t_i)$ is

$$
\begin{aligned}
\frac{\partial}{\partial q(t_i)} & R(q(t_i))a_r(t_i)\Delta t_{i+1} \\
&= \lim_{\theta \to 0} \frac{1}{\theta} \left\{ R(q(t_i) + \theta)a_r(t_i) - R(q(t_i))a_r(t_i) \right\} \Delta t \\
&= \lim_{\theta \to 0} \frac{1}{\theta} \left\{ R(q(t_i))\mathrm{Exp}(\theta)a_r(t_i) - R(q(t_i))a_r(t_i) \right\} \Delta t \\
&= \lim_{\theta \to 0} \frac{1}{\theta} \left\{ R(q(t_i))(I + [\theta]_\times)a_r(t_i) - R(q(t_i))a_r(t_i) \right\} \Delta t \\
&= \lim_{\theta \to 0} \frac{1}{\theta} \left\{ R(q(t_i)) [\theta]_\times \, a_r(t_i) \right\} \Delta t \\
&= \lim_{\theta \to 0} \frac{1}{\theta} \left\{ -R(q(t_i)) [a_r(t_i)]_\times \theta \right\} \Delta t \\
&= -R(q(t_i)) [a_r(t_i)]_\times \Delta t_{i+1}.
\end{aligned}
$$
(49)

Removing Δt_{i+1} from $R(q(t_i))\left\{ V(t_i)R^T(q(t_i))v(t_i) \right\} \Delta t_{i+1}$ of (46), and differentiating it with respect to $q(t_i)$ yields

$$
\begin{aligned}
\frac{\partial}{\partial q(t_i)} & R(q(t_i))\left\{ V(t_i)R^T(q(t_i))v(t_i) \right\} \\
&= \frac{\partial}{\partial q} R(q)\left\{ VR^T(q)\, v \right\} \\
&= \frac{\partial}{\partial q} \left\{ R(q)\, VR^T(q)\, v \right\} \\
&= \lim_{\theta \to 0} \frac{1}{\theta} \left\{ \left(R(q + \theta)VR^T(q + \theta)v \right) \right. \\
&\quad \left. - \left(R(q)VR^T(q)\, v \right) \right\} \\
&= \lim_{\theta \to 0} \frac{1}{\theta} \left\{ \left(R(q)\mathrm{Exp}(\theta)V\, (R(q)\mathrm{Exp}(\theta))^T\, v \right) \right. \\
&\quad \left. - \left(R(q)VR^T(q)\, v \right) \right\} \\
&= \lim_{\theta \to 0} \frac{1}{\theta} \left\{ \left(R(q)(I + [\theta]_\times)V\, (R(q)(I + [\theta]_\times))^T\, v \right) \right. \\
&\quad \left. - \left(R(q)VR^T(q)\, v \right) \right\} \\
&= \lim_{\theta \to 0} \frac{1}{\theta} \left\{ \left(R(q)(I + [\theta]_\times)V\, \left((I + [\theta]_\times)^T R^T(q) \right) v \right) \right. \\
&\quad \left. - \left(R(q)VR^T(q)\, v \right) \right\} \\
&= \lim_{\theta \to 0} \frac{1}{\theta} \left\{ \left(R(q)(I + [\theta]_\times)V\, \left((I^T + [\theta]_\times^T)R^T(q) \right) v \right) \right. \\
&\quad \left. - \left(R(q)VR^T(q)\, v \right) \right\}
\end{aligned}
$$

$$
\begin{aligned}
&= \lim_{\theta \to 0} \frac{1}{\theta} \left\{ \left(\boldsymbol{R}(q)(\boldsymbol{I} + [\theta]_\times) \boldsymbol{V} \left((\boldsymbol{I} - [\theta]_\times) \boldsymbol{R}^T(q) \right) \boldsymbol{v} \right) \right. \\
&\qquad \left. - \left(\boldsymbol{R}(q) \boldsymbol{V} \boldsymbol{R}^T(q) \, \boldsymbol{v} \right) \right\} \\
&= \lim_{\theta \to 0} \frac{1}{\theta} \left\{ \boldsymbol{R}(q) [\theta]_\times \boldsymbol{V} \boldsymbol{R}^T(q) \, \boldsymbol{v} \right. \\
&\qquad \left. - \boldsymbol{R}(q) \boldsymbol{V} [\theta]_\times \boldsymbol{R}^T(q) \, \boldsymbol{v} - \boldsymbol{R}(q) [\theta]_\times \boldsymbol{V} [\theta]_\times \boldsymbol{R}^T(q) \, \boldsymbol{v} \right\} \\
&= \lim_{\theta \to 0} \frac{1}{\theta} \left\{ -\boldsymbol{R}(q) \left[\boldsymbol{V} \boldsymbol{R}^T(q) \, \boldsymbol{v} \right]_\times \theta \right. \\
&\qquad \left. + \boldsymbol{R}(q) \boldsymbol{V} \left[\boldsymbol{R}^T(q) \, \boldsymbol{v} \right]_\times \theta + \boldsymbol{R}(q) \left[\boldsymbol{V} [\theta]_\times \boldsymbol{R}^T(q) \, \boldsymbol{v} \right]_\times \theta \right\} \\
&= -\boldsymbol{R}(q) \left[\boldsymbol{V} \boldsymbol{R}^T(q) \, \boldsymbol{v} \right]_\times + \boldsymbol{R}(q) \boldsymbol{V} \left[\boldsymbol{R}^T(q) \, \boldsymbol{v} \right]_\times \\
&\qquad + \lim_{\theta \to 0} \boldsymbol{R}(q) \left[\boldsymbol{V} [\theta]_\times \boldsymbol{R}^T(q) \, \boldsymbol{v} \right]_\times \\
&= -\boldsymbol{R}(q) \left[\boldsymbol{V} \boldsymbol{R}^T(q) \, \boldsymbol{v} \right]_\times + \boldsymbol{R}(q) \boldsymbol{V} \left[\boldsymbol{R}^T(q) \, \boldsymbol{v} \right]_\times \\
&\qquad + \lim_{\theta \to 0} \boldsymbol{R}(q) \left[-\boldsymbol{V} \left[\boldsymbol{R}^T(q) \, \boldsymbol{v} \right]_\times \theta \right]_\times \\
&= -\boldsymbol{R}(q) \left[\boldsymbol{V} \boldsymbol{R}^T(q) \, \boldsymbol{v} \right]_\times + \boldsymbol{R}(q) \boldsymbol{V} \left[\boldsymbol{R}^T(q) \, \boldsymbol{v} \right]_\times + \boldsymbol{0}_3. \quad (50)
\end{aligned}
$$

Combining (46), (49), and (50) yields $\frac{\partial \boldsymbol{v}(t_{i+1})}{\partial q(t_i)}$ as follows:

$$
\frac{\partial \boldsymbol{v}(t_{i+1})}{\partial q(t_i)} = -\boldsymbol{R} \left\{ [\boldsymbol{a}_r]_\times + \left[\boldsymbol{V} \boldsymbol{R}^T \boldsymbol{v} \right]_\times - \boldsymbol{V} \left[\boldsymbol{R}^T \boldsymbol{v} \right]_\times \right\} \Delta t. \tag{51}
$$

B. PARTIAL DERIVATIVES OF ATTITUDE

$q(t_i)$ propagates during the time interval Δt_{i+1} to $q(t_{i+1})$ according to the following equation, which is derived from (7) using Lie group theory:

$$
\begin{aligned}
q(t_{i+1}) &= q(t_i) \otimes \mathrm{Exp}(\boldsymbol{\omega}(t_i) \Delta t_{i+1}) \\
&= q(t_i) \otimes \begin{bmatrix} \cos\left(\|\boldsymbol{\omega}(t_i)\| \dfrac{\Delta t_{i+1}}{2} \right) \\[2mm] \dfrac{\boldsymbol{\omega}(t_i)}{\|\boldsymbol{\omega}(t_i)\|} \sin\left(\|\boldsymbol{\omega}(t_i)\| \dfrac{\Delta t_{i+1}}{2} \right) \end{bmatrix}. \quad (52)
\end{aligned}
$$

From (52), the partial derivatives of $q(t_{i+1})$ with respect to $q(t_i)$ and $\boldsymbol{\omega}(t_i)$ are obtained as follows [2], [20]:

$$
\frac{\partial q(t_{i+1})}{\partial q(t_i)} = \boldsymbol{R}^T(\boldsymbol{\omega} \Delta t), \tag{53}
$$

$$
\begin{aligned}
\frac{\partial q(t_{i+1})}{\partial \boldsymbol{\omega}(t_i)} &= \left(\boldsymbol{I}_3 - \frac{1 - \cos \|\boldsymbol{r}\|}{\|\boldsymbol{r}\|^2} [\boldsymbol{r}]_\times \right. \\
&\qquad \left. + \frac{\|\boldsymbol{r}\| - \sin \|\boldsymbol{r}\|}{\|\boldsymbol{r}\|^3} [\boldsymbol{r}]_\times^2 \right) \Delta t. \tag{54}
\end{aligned}
$$

REFERENCES

[1] M. Arnold, A. Cardona, and O. Brüls, "A lie algebra approach to lie group time integration of constrained systems," in *Structure-Preserving Integrators in Nonlinear Structural Dynamics and Flexible Multibody Dynamics* (CISM International Centre for Mechanical Sciences), vol. 565, P. Betsch, Ed. Cham, Switzerland: Springer, 2016, pp. 91–158.

[2] J. Solà, "Quaternion kinematics for the error-state Kalman filter," 2017, *arXiv:1711.02508.*

[3] A. Müller, "Group theoretical approaches to vector parameterization of rotations," *J. Geometry Symmetry Phys.*, vol. 19, pp. 43–72, Jan. 2010.

[4] M. Greiff, Z. Sun, and A. Robertsson, "Attitude control on SU(2): Stability, robustness, and similarities," *IEEE Control Syst. Lett.*, vol. 6, pp. 73–78, 2021.

[5] F. L. Markley, "Attitude error representations for Kalman filtering," *J. Guid., Control, Dyn.*, vol. 26, no. 2, pp. 311–317, Mar./Apr.2003.

[6] E. J. Lefferts, F. L. Markley, and M. D. Shuster, "Kalman filtering for spacecraft attitude estimation," *J. Guid., Control, Dyn.*, vol. 5, no. 5, pp. 417–429, 1982.

[7] M. D. Shuster and S. D. Oh, "Three-axis attitude determination from vector observations," *J. Guid. Control, Dyn.*, vol. 4, no. 1, pp. 70–77, Jan. 1981.

[8] A. Barrau and S. Bonnabel, "The invariant extended Kalman filter as a stable observer," *IEEE Trans. Autom. Control*, vol. 62, no. 4, pp. 1797–1812, Apr. 2017.

[9] K. S. Phogat and E. C. Dong, "Invariant extended Kalman filter on matrix Lie groups," *Automatica*, vol. 114, pp. 11–23, Apr. 2020.

[10] A. Barrau and S. Bonnabel, "Invariant Kalman filtering," *Annu. Rev. Control, Robot., Auton. Syst.*, vol. 1, pp. 237–257, May 2018.

[11] N. Ko, W. Youn, I. Choi, G. Song, and T. Kim, "Features of invariant extended Kalman filter applied to unmanned aerial vehicle navigation," *Sensors*, vol. 18, no. 9, p. 2855, Aug. 2018.

[12] M. Brossard, A. Barrau, P. Chauchat, and S. Bonnabel, "Associating uncertainty to extended poses for on lie group IMU preintegration with rotating earth," *IEEE Trans. Robot.*, vol. 38, no. 2, pp. 998–1015, Apr. 2022.

[13] M. R. Cohen and J. R. Forbes, "Navigation and control of unconventional VTOL UAVs in forward-flight with explicit wind velocity estimation," *IEEE Robot. Autom. Lett.*, vol. 5, no. 2, pp. 1151–1158, Apr. 2020.

[14] M. Wang and A. Tayebi, "Hybrid nonlinear observers for inertial navigation using landmark measurements," *IEEE Trans. Autom. Control*, vol. 65, no. 12, pp. 5173–5188, Dec. 2020.

[15] H. A. Hashim, "GPS-denied navigation: Attitude, position, linear velocity, and gravity estimation with nonlinear stochastic observer," in *Proc. Amer. Control Conf. (ACC)*, New Orleans, LA, USA, May 2021, pp. 1149–1154, doi: 10.23919/ACC50511.2021.9482995.

[16] G. Bourmaud, R. Mégret, A. Giremus, and Y. Berthoumieu, "Discrete extended Kalman filter on Lie groups," in *Proc. 21st Eur. Signal Process. Conf. (EUSIPCO)*, Marrakech, Morocco, Sep. 2013, pp. 1–5.

[17] G. Bourmaud, R. Mégret, M. Arnaudon, and A. Giremus, "Continuous-discrete extended Kalman filter on matrix lie groups using concentrated Gaussian distributions," *J. Math. Imag. Vis.*, vol. 51, no. 1, pp. 209–228, Jan. 2015.

[18] H. A. Hashim and A. E. E. Eltoukhy, "Nonlinear filter for simultaneous localization and mapping on a matrix lie group using IMU and feature measurements," *IEEE Trans. Syst., Man, Cybern., Syst.*, vol. 52, no. 4, pp. 2098–2109, Apr. 2022, doi: 10.1109/TSMC.2020.3047338.

[19] F. Pei, S. Yang, and S. Yin, "In-motion initial alignment using state-dependent extended Kalman filter for strapdown inertial navigation system," *IEEE Trans. Instrum. Meas.*, vol. 70, pp. 1–12, 2020, doi: 10.1109/TIM.2020.3027405.

[20] J. Solà, J. Deray, and D. Atchuthan, "A micro lie theory for state estimation in robotics," 2018, *arXiv:1812.01537.*

[21] J. Cui, M. Wang, W. Wu, and X. He, "Lie group based nonlinear state errors for MEMS-IMU/GNSS/magnetometer integrated navigation," *J. Navigat.*, vol. 74, no. 4, pp. 887–900, Jul. 2021, doi: 10.1017/S037346332100014X.

[22] M. Brossard, S. Bonnabel, and A. Barrau, "Unscented Kalman filter on lie groups for visual inertial odometry," in *Proc. IEEE/RSJ Int. Conf. Intell. Robots Syst. (IROS)*, Madrid, Spain, Oct. 2018, pp. 649–655, doi: 10.1109/IROS.2018.8593627.

[23] M. Brossard, S. Bonnabel, and J.-P. Condomines, "Unscented Kalman filtering on lie groups," in *Proc. IEEE/RSJ Int. Conf. Intell. Robots Syst. (IROS)*, Vancouver, BC, Canada, Sep. 2017, pp. 2485–2491, doi: 10.1109/IROS.2017.8206066.

[24] M. Brossard, A. Barrau, and S. Bonnabel, "A code for unscented Kalman filtering on manifolds (UKF-M)," in *Proc. IEEE Int. Conf. Robot. Autom. (ICRA)*, Paris, France, May 2020, pp. 5701–5708, doi: 10.1109/ICRA40945.2020.9197489.

[25] B. Xie and S. Dai, "A comparative study of extended Kalman filtering and unscented Kalman filtering on lie group for stewart platform state estimation," in *Proc. 6th Int. Conf. Control Robot. Eng. (ICCRE)*, Beijing, China, Apr. 2021, pp. 145–150, doi: 10.1109/ICCRE51898.2021.9435722.

[26] H. Guo, H. Liu, Y. Zhou, and J. Li, "Quaternion invariant cubature Kalman filtering for attitude estimation," in *Proc. 3rd World Conf. Mech. Eng. Intell. Manuf. (WCMEIM)*, Shanghai, China, Apr. 2021, pp. 67–72, doi: 10.1109/WCMEIM52463.2020.00020.

[27] N. Y. Ko, I. H. Choi, G. Song, and W. Youn, "Three-dimensional dynamic-model-aided navigation of multirotor unmanned aerial vehicles," *IEEE Access*, vol. 7, pp. 170715–170732, 2019, doi: 10.1109/ACCESS.2019.2955756.

[28] D. Abeywardena, S. Kodagoda, G. Dissanayake, and R. Munasinghe, "Improved state estimation in quadrotor MAVs: A novel drift-free velocity estimator," *IEEE Robot. Autom. Mag.*, vol. 20, no. 4, pp. 32–39, Dec. 2013, doi: 10.1109/MRA.2012.2225472.

[29] M. Khaghani and J. Skaloud, "Assessment of VDM-based autonomous navigation of a UAV under operational conditions," *Robot. Auton. Syst.*, vol. 106, pp. 152–164, Aug. 2018.

[30] R. Mahony, V. Kumar, and P. Corke, "Multirotor aerial vehicles: Modeling, estimation, and control of quadrotor," *IEEE Robot. Autom. Mag.*, vol. 19, no. 3, pp. 20–32, Sep. 2012.

[31] British Geological Survey. *World Magnetic Model 2020 Calculator*. Accessed: Jan. 19, 2022. [Online]. Available: http://www.geomag.bgs.ac.uk/data_service /models_compass/wmm_calc.html

[32] C. T. Kelley, "Nonlinear least squares," in *Iterative Methods for Optimization*. Philadelphia, PA, USA: SIAM, 1999, ch. 2, sec. 4, pp. 22–27.

[33] Dronecode Foundation. *Using ECL EKF, PX4 User Guide*. Accessed: May 24, 2021. [Online]. Available: https://docs.px4.io/master/en/advanced _config/tuning_the_ecl_ekf.html

[34] S. Bonnabel, P. Martin, and E. Salaün, "Invariant extended Kalman filter: Theory and application to a velocity-aided attitude estimation problem," in *Proc. 48th IEEE Conf. Decision Control (CDC)*, Shanghai, China, Dec. 2009, pp. 1297–1304.

GYEONGSUB SONG received the B.S. and M.S. degrees from the Department of Control, Instrumentation, and Robot Engineering, Chosun University, Gwangju, South Korea, in 2016 and 2018, respectively, where he is currently pursuing the Ph.D. degree in robotics and the navigation of unmanned aerial vehicles with the Department of Control and Instrumentation Engineering.

He has worked on estimation and filtering of parameters related to the navigation of unmanned vehicles. His research interests include the navigation of unmanned aerial and underwater vehicles.

WONKEUN YOUN (Member, IEEE) received the B.S. degree from Handong Global University, Pohang, South Korea, in 2008, and the M.S. degree in mechanical engineering and the Ph.D. degree in robotics from the Korea Advanced Institute of Science and Technology (KAIST), Daejeon, South Korea, in 2010 and 2020, respectively.

From 2011 to 2021, he was a Senior Researcher with the Unmanned Aircraft System Research Division, Korea Aerospace Research Institute (KARI). Since 2021, he has been an Assistant Professor with Chungnam National University. His current research interests include multisensor fusion, Bayesian estimation theory, multimodal target tracking, and GPS/INS-based navigation.

NAK YONG KO (Member, IEEE) received the B.S., M.S., and Ph.D. degrees from the Department of Control and Instrumentation Engineering, Seoul National University, Seoul, South Korea, in 1985, 1987, and 1993, respectively.

He has been a Professor with the Department of Electronic Engineering, Chosun University, Gwangju, South Korea, since 1992. He has worked as a Visiting Research Scientist with The Robotics Institute, Carnegie Mellon University, Pittsburgh, PA, USA, from 1997 to 1998 and from 2004 to 2005. He is involved in projects developing unmanned aerial vehicles and underwater vehicles, especially in the development of navigation algorithms. His research interests include navigation, collision avoidance, and motion planning in robotics.

Prof. Ko is a member of IEEE Robotics and Automation Society and Oceanic Engineering Society and a member of the Institute of Control, Robotics and Systems, South Korea.

SUNG HYUN YOU received the B.S. degree in electrical engineering from the Seoul National University of Science and Technology, Seoul, South Korea, in 2013, and the Ph.D. degree from the School of Electrical Engineering, Korea University, Seoul, in 2019.

He was a Research Professor with the Research Institute of Engineering and Technology, Korea University. Since 2020, he has been an Assistant Professor with Chosun University, South Korea. His research interests include optimal, robust, intelligent, and receding horizon controls and estimations.